

# Stabilizing Phase-balanced or Phase-synchronized Trajectories of Van der Pol Oscillators in Uniform Electrical Networks

Mohit Sinha, F. Dörfler, B. Johnson, and Sairaj Dhople

**Abstract**—We study the dynamics of Van der Pol oscillators in a class of electrical networks with the goal of synthesizing feedback strategies to stabilize either phase-synchronized or phase-balanced motions. The electrical networks are composed of transmission lines with series  $R$ - $L$  circuit models that are uniform, by which we mean that the  $R$ -to- $L$  ratios of all lines are the same. The oscillators are coupled through linear filters on their output currents to nodes in the network. Our main results illustrate how the signs of the local feedback gains determine the stability of either phase-synchronized or phase-balanced trajectories. The results have implications on (and indeed, the paper is motivated by) decentralized control of power converters: synchronized solutions are of interest in parallel-connected dc-ac inverters and phase-balanced solutions are of interest in interleaving switching waveforms for multiphase dc-dc converters.

## I. INTRODUCTION

Problems pertaining to modeling, analyzing, and controlling nonlinear oscillators in complex networks continue to garner attention in a variety of scientific disciplines [1]. Recent efforts where the dynamics of nonlinear oscillators are leveraged in electrical-engineering applications (and are aligned with the theoretical underpinnings of this work) include: realizing controllers for power converters [2]–[6] and phase-based computation [7]–[9]. While synchronization typically receives the bulk of the attention in complex networks of nonlinear oscillators, the phenomenon called phase balancing, where phases evolve spaced out such that the centroid of the coupled oscillators (when conceptualized to be moving points on a circle) is at the origin, is equally intriguing from theoretical and application vantage points.

In this paper, we examine the dynamics of Van der Pol oscillators connected in uniform electrical networks with transmission lines modeled as series  $R$ - $L$  circuits. By uniform electrical networks, we mean that the  $R$ -to- $L$  ratios of all lines are the same. The oscillators are coupled through a linear filter on their output currents to the network. This setup underlies two decentralized-control applications in networks of power-electronics circuits that we have examined previously: real-time synchronization of ac outputs of parallel inverters [3] and interleaving of switching waveforms in dc-dc converter systems [10]. For each application, we encode the dynamics of the nonlinear oscillators on to the micro-controllers for the power converters to realize the controllers. The dynamics of the nonlinear oscillators drive the behavior of the power converters to the desired operating condition (synchronization in the ac application and interleaving in the dc application). It so emerges that the sign of the feedback gain fundamentally dictates the nature of equilibria

in such settings. A systematically designed *negative* feedback stabilizes sinusoidal oscillations that are phase synchronized (of interest in the ac case). Conversely, when the feedback gain is *positive*, one can stabilize phase-balanced sinusoidal oscillations (of interest in the dc application).

The controller dynamics—those of the nonlinear Van der Pol oscillator—and the nature of the electrical network—with uniform lines—are common to both applications. This motivates us to develop a unified theoretical lens to examine (the admittedly fundamentally different) phase-synchronized and phase-balanced motions in uniform electrical networks of Van der Pol oscillator circuits. This work builds on and attempts to unify our previous efforts that have disparately investigated synchronization and balancing conditions for phase dynamics of nonlinear oscillator circuits. In [11], [12], we examined synchronization conditions for Liénard-type oscillators (a general class of nonlinear oscillators to which Van der Pol oscillators belong) in heterogeneous electrical networks (no assumptions on uniformity of  $R$ -to- $L$  ratios). In [13], we explored conditions for phase balancing in static all-to-all coupled networks of Liénard-type oscillators. The setting in this work significantly broadens the scope of our previous examination of phase-balanced motion [13] (since we examine more general network topologies with dynamics here) but is admittedly limited when compared to our work on phase-synchronized motion [11], [12] (since we focus on the special class of uniform networks here). Nonetheless, the setup in this paper is a common denominator to both settings discussed above, and we therefore focus our investigations accordingly. We also bring to attention work such as [14], [15], where synchronization and balancing are studied with a unified perspective for Kuramoto oscillators and planar kinematic models, respectively. The scope of our efforts and implication of our results are different, given: i) the more complex nonlinear dynamics that emerge from the circuit models of the Van der Pol oscillators, and ii) the nature of the network and feedback that are motivated by the application domain of power-electronics circuits.

To establish the conditions for stabilization of the desired phase-balanced and phase-synchronized equilibria, we leverage Lyapunov, averaging, and linearization based arguments. To facilitate analysis of the coupled oscillators, we translate the dynamics that derive from circuit laws to a time-autonomous system leveraging the weakly nonlinear time-periodic nature of the dynamics and the theory of averaging [16]–[18]. The averaged model dynamics, so obtained, lend itself to a gradient flow formulation which we

then use to invoke Lyapunov and LaSalle invariance-based arguments to establish convergence to the stationary points of the system. Finally, we study when the phase-balanced and phase-synchronous set exist at equilibrium and establish their local exponential stability.

The remainder of this paper is organized as follows. Section II introduces mathematical preliminaries and the coupled nonlinear oscillator model. Building upon this, Section III outlines the nature of the solutions of the system and the local stability of the equilibria of interest (i.e., phase-balanced and phase-synchronous trajectories). We validate our analysis through numerical simulations in Section IV and conclude with some suggestions for future work in Section V.

## II. PRELIMINARIES AND SYSTEM MODEL

In this section, we build a dynamical-system model for the network of nonlinear oscillator circuits. We begin by discussing the nonlinear oscillator model and then describe the attributes of the electrical network. First, we summarize mathematical notation that is used in the paper.

### A. Notation

The  $N$ -dimensional space of non-negative real numbers is denoted by  $\mathbb{R}_{\geq 0}^N$  and  $\mathbb{T}^N$  denotes the  $N$ -dimensional torus. For a matrix  $X$ ,  $\lambda_{\max}(X)$  returns the maximum of its eigenvalues,  $X_{jk}$  represents the entry in its  $j$ -th row and  $k$ -th column, and  $X_{\text{diag}}$  is a vector with all the diagonal entries. Finally,  $\max(X)$  returns the maximum entry of vector  $X$ ,  $j := \sqrt{-1}$ ,  $0_N$  denotes the vector of all zeros,  $1_N$  denotes the vector of all ones, and  $I_N$  denotes the  $N \times N$  identity matrix.

### B. Van der Pol Oscillator Circuit

The circuit model of the Van der Pol oscillator contains the parallel connection of: i) a harmonic oscillator with inductance,  $L$ , and capacitance,  $C$  (yielding a resonant frequency,  $\omega = 1/\sqrt{LC}$ ), ii) a negative-conductance element,  $-\sigma$ , and iii) a cubic voltage-dependent current source. (See Fig. 1 for a circuit diagram of the oscillator.)

The dynamics of the  $j$ th oscillator circuit are given by:

$$L \frac{di_{Lj}}{dt} = v_{Cj}, \quad (1)$$

$$C \frac{dv_{Cj}}{dt} = -i_{Lj} - (\sigma v_{Cj} - \alpha v_{Cj}^3) + i_j, \quad (2)$$

where  $v_{Cj}$  is the capacitor voltage,  $i_{Lj}$  is the current through the inductor, and  $i_j$  is the input current into the oscillator. Now, defining  $\varepsilon := \sqrt{L/C}$ , we put the system into the following state-space form with  $x_j = \varepsilon i_{Lj}$  and  $y_j = v_{Cj}$  adopted as states:

$$\frac{dx_j}{dt} = \omega y_j, \quad (3)$$

$$\frac{dy_j}{dt} = -\omega x_j + \varepsilon \omega (\sigma y_j - \alpha y_j^3) + \varepsilon \omega i_j. \quad (4)$$

In subsequent developments, we assume  $\varepsilon \ll 1$ , which yields near-sinusoidal oscillations. Furthermore, with the above formulation, the weak coupling through the input is obvious.

### C. Electrical Network

We study the trajectories of  $N$  identical nonlinear oscillator circuits described above, which are indexed by elements in the set  $\mathcal{N} := \{1, \dots, N\}$ . The oscillators are connected over an electrical network modeled as an undirected graph with edges corresponding to the electrical transmission lines collected in the set  $\mathcal{E} \subseteq \mathcal{N} \times \mathcal{N}$ . The electrical lines are modeled with series  $R$ - $L$  circuits. The network is assumed to be *uniform*, by which we mean that all the lines have the same  $R$ -to- $L$  ratio, which we denote by  $\gamma$ .

### D. Nature of Feedback

We construct the following feedback for the oscillators through input currents  $i = [i_1, \dots, i_N]^T$ :

$$i = \kappa Y v_C, \quad (5)$$

where  $v_C = [v_{C,1}, \dots, v_{C,N}]^T$  and  $\kappa$  is the feedback gain. Entries of the (admittance-like) matrix  $Y \in \mathbb{R}^{N \times N}$  are:

$$Y_{jk} = \begin{cases} -\frac{1}{L_{jk}} & \text{if } j \neq k \text{ and } (j, k) \in \mathcal{E} \\ 0 & \text{if } j \neq k \text{ and } (j, k) \notin \mathcal{E} \\ -\sum_{\ell=1, \ell \neq j}^N Y_{j\ell} & \text{if } j = k \end{cases} \quad (6)$$

We note that  $Y$  is a weighted Laplacian matrix and is therefore positive semidefinite. The feedback law in (5) corresponds to the setting where the currents injected into the electrical network at the nodes with oscillators are filtered by the linear filter  $\kappa(s + \gamma)$ , with the filtered versions then injected into each oscillator.<sup>1</sup> Figure 2 illustrates the setup.

With the feedback in (5), the oscillator dynamics in (3)–(4) can be collectively represented as:

$$\dot{x} = \omega y, \quad (7)$$

$$\dot{y} = -\omega x + \varepsilon \omega (F(y) + \kappa Y y), \quad (8)$$

where  $x = [x_1, \dots, x_N]^T$ ,  $y = [y_1, \dots, y_N]^T$  collect the states of the  $N$  oscillators, and  $F(y) := [\sigma y_1 - \alpha y_1^3, \dots, \sigma y_N - \alpha y_N^3]^T$ .

### E. Dynamical-systems Model for Coupled Oscillators

Consider the following bijective coordinate transformation from the state-space model in (3)–(4) to polar coordinates:

$$x_j \rightarrow r_j \sin(\omega t + \theta_j), \quad y_j \rightarrow r_j \cos(\omega t + \theta_j). \quad (9)$$

<sup>1</sup>To see this, observe that dynamics on the  $R$ - $L$  lines are such that the currents injected into the network are given by  $(s + \gamma)^{-1} Y v_C$ .

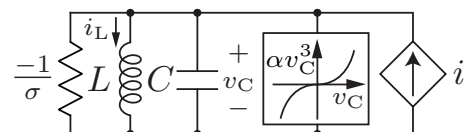


Fig. 1: Circuit diagram of a Van der Pol oscillator.

In these new set of coordinates, the amplitude and phase dynamics of the  $j$ -th oscillator are given by:

$$\begin{aligned} \dot{r}_j &= \varepsilon\omega (\sigma r_j \cos^2(\omega t + \theta_j) - \alpha r_j^3 \cos^4(\omega t + \theta_j)) \\ &\quad + \varepsilon\omega i_j \cos(\omega t + \theta_j), \end{aligned} \quad (10)$$

$$\begin{aligned} \dot{\theta}_j &= \frac{\varepsilon\omega}{2} (\sigma r_j - \alpha r_j^3 \cos^2(\omega t + \theta_j)) \sin(2\omega t + \theta_j) \\ &\quad + \varepsilon\omega i_j \sin(\omega t + \theta_j). \end{aligned} \quad (11)$$

Using the method of periodic averaging,<sup>2</sup> the amplitude and phase dynamics of the non-autonomous system above in (10)–(11) are approximated by:

$$\begin{aligned} \dot{\bar{r}}_j &= \frac{\varepsilon\omega^2}{2\pi} \int_0^{2\pi} (\sigma - \alpha \bar{r}_j^2 \cos^2(\omega t + \bar{\theta}_j)) \bar{r}_j \cos^2(\omega t + \bar{\theta}_j) dt \\ &\quad + \frac{\kappa\varepsilon\omega^2}{2\pi} \int_0^{2\pi} \sum_{k=1}^N Y_{jk} \bar{r}_k \cos(\omega t + \bar{\theta}_k) \cos(\omega t + \bar{\theta}_j) dt, \\ \dot{\bar{\theta}}_j &= \frac{\varepsilon\omega^2}{4\pi} \int_0^{2\pi} (\sigma - \alpha \bar{r}_j^2 \cos^2(\omega t + \bar{\theta}_j)) \sin(2\omega t + \bar{\theta}_j) dt \\ &\quad + \frac{\kappa\varepsilon\omega^2}{2\pi \bar{r}_j} \int_0^{2\pi} \sum_{k=1}^N Y_{jk} \bar{r}_k \cos(\omega t + \bar{\theta}_k) \sin(\omega t + \bar{\theta}_j) dt, \end{aligned}$$

where we have substituted for inputs  $i_j$  from (5). Evaluating the integrals and ignoring the  $\mathcal{O}(\varepsilon^2)$  terms yields the time-autonomous system:

$$\dot{\bar{r}}_j = \varepsilon\omega \left( \frac{\sigma \bar{r}_j}{2} - \frac{3\alpha \bar{r}_j^3}{8} \right) + \frac{\varepsilon\omega\kappa}{2} \sum_{k=1}^N Y_{jk} \bar{r}_k \cos(\bar{\theta}_{jk}), \quad (12)$$

$$\dot{\bar{\theta}}_j = -\frac{\varepsilon\omega\kappa}{2\bar{r}_j} \sum_{k=1}^N Y_{jk} \bar{r}_k \sin(\bar{\theta}_{jk}), \quad (13)$$

where we define  $\bar{\theta}_{jk} := \bar{\theta}_j - \bar{\theta}_k$ .

### III. NATURE AND STABILITY OF SOLUTIONS

In this section, we study the nature of the trajectories of the coupled oscillator circuits with the proposed designed

<sup>2</sup>Consider a time-varying dynamical system  $\dot{x} = \varepsilon h(x, t, \varepsilon)$ , where  $h(x, t, \varepsilon) = h(x, t + T, \varepsilon)$  with (period)  $T > 0$ , and  $0 < \varepsilon \ll 1$ . The solution to this system can be approximated up to  $\mathcal{O}(\varepsilon)$  by that of the averaged system  $\dot{\bar{x}} = \varepsilon \bar{h}(\bar{x}) = \varepsilon \frac{1}{T} \int_{\tau=0}^T h(\bar{x}, \tau, 0) d\tau$ .

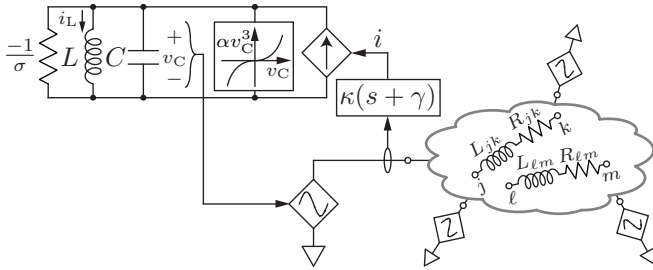


Fig. 2: Illustration of circuit diagram of Van der Pol oscillator and interconnection to electrical network. The electrical network is uniform, with all transmission lines having the same  $R$ -to- $L$  ratio, i.e.,  $R_{jk}/L_{jk} = R_{lm}/L_{lm} =: \gamma$ . The oscillators are interfaced to the network through filters  $\kappa(s + \gamma)$ .

feedback. First, we define the two sets of equilibria we seek to stabilize.

**Definition 1 (Phase-synchronous Set).** *The set that describes the phase-synchronized collective motion with the oscillators having the same radii is called the phase synchronous set,  $\mathcal{S}$ :*

$$\mathcal{S} := \{\bar{r}_j = \bar{r}_k, \bar{\theta}_{jk} = 0 \pmod{2\pi}, \forall j, k \in \mathcal{N}\}. \quad (14)$$

We will find that with  $\kappa < 0$ , we can guarantee the local exponential stability of phase-synchronized equilibria.

**Definition 2 (Phase-balanced Set).** *The set that describes collective motion where the centroid of the coupled oscillator system is at the origin and the oscillator dynamics have the same radii on the polar plane is called the phase-balanced set,  $\mathcal{B}$ :*

$$\mathcal{B} := \{\bar{r}_j = \bar{r}_k, \sum_{k=1}^N e^{j\bar{\theta}_k} = 0, \forall j, k \in \mathcal{N}\}. \quad (15)$$

We will subsequently show that with  $\kappa > 0$ , we can guarantee local exponential stability of phase-balanced equilibria.

#### A. Well-posedness of Dynamics

We first demonstrate that the trajectories returned by the dynamical system (12)–(13) are always such that the radii are well defined, i.e.,  $\bar{r}_j > 0, \forall j \in \mathcal{N}$ , and phases  $\bar{\theta}_j \in \mathbb{T}^N$ . We establish this next.

**Lemma 1.** *If the following condition holds:*

$$\sigma > -\kappa\lambda_{\max}(Y), \quad (16)$$

then, the set

$$\mathcal{I} := \{(\bar{r}, \bar{\theta}) \in \mathbb{R}_{\geq 0}^N \times \mathbb{T}^N : \bar{r}_j > 0, \forall j \in \mathcal{N}\} \quad (17)$$

is positively invariant under the flow (12)–(13).

*Proof.* The Jacobian of (7)–(8) around the origin is given by:

$$\begin{bmatrix} 0_{N \times N} & \omega I_N \\ -\omega I_N & \varepsilon\omega (\sigma I_N + \kappa Y) \end{bmatrix}, \quad (18)$$

where  $\varepsilon\omega (\sigma I_N + \kappa Y)$  is a diagonally dominant matrix with positive diagonal entries and is therefore positive definite if  $\sigma > -\kappa\lambda_{\max}(Y)$ . Let the set  $\{\lambda_1, \dots, \lambda_N\}$  denote eigenvalues of  $\varepsilon\omega (\sigma I_N + \kappa Y)$  (it is worth pointing out that the symmetry of  $(\sigma I_N + \kappa Y)$  induces  $\lambda_j \in \mathbb{R}, \forall j = 1, \dots, N$ ), then the  $2N$  eigenvalues of the Jacobian are of the form  $0.5(\lambda_j \pm (\lambda_j^2 - 4\omega^2)^{\frac{1}{2}}), j = 1, \dots, N$ . Thus, all the eigenvalues of the Jacobian have positive real parts if  $\sigma > -\kappa\lambda_{\max}(Y)$ , and hence the origin is repulsive.

Since the transformation (9) is bijective (for  $r_j > 0$ ), repulsiveness of the origin of system (7)–(8) implies that  $r_j(t) \neq 0, \forall t \geq 0$  if  $r_j(0) \neq 0, \forall j \in \mathcal{N}$ . Now, going back to the averaged system, note that we have  $\forall t > 0$

$$\bar{r}_j(t) = \frac{\omega}{2\pi} \int_{\tau=t-2\pi/\omega}^t r_j(\tau) d\tau, \quad (19)$$

with  $\bar{r}_j(0) = r_j(0)$ . So,  $\bar{r}_j(0) > 0$ , which implies  $r_j(0) > 0$ , leads to trajectories such that  $r_j(t) > 0, \forall t \geq 0$ . Finally,  $\bar{r}_j = 0$  if and only if there exists an interval  $[t_1, t_2]$  of length greater than the period, i.e.,  $|t_2 - t_1| \geq 2\pi/\omega$  such that  $r_j(t) = 0$  for  $t \in [t_1, t_2]$  because  $r_j(t)$  is nonnegative and  $2\pi/\omega$ -periodic, and hence  $r_j(t) > 0, \forall t \geq 0$  implies  $\bar{r}_j(t) > 0, \forall t \geq 0$ . Therefore, the set  $\mathcal{I}$  is positively invariant. ■

### B. Convergence to Equilibria

Now, we use the averaged model in (12)–(13) to study the nature of the trajectories of the collective motion. First, we investigate convergence to the equilibria with a Lyapunov-based argument.

**Theorem 1 (Convergence of Oscillator Dynamics).** *Consider the collective motion of the  $N$  identical oscillators, with the dynamics of each described by the flow (12)–(13), and assume  $\sigma > -\kappa\lambda_{\max}(Y)$  to guarantee the positive invariance of set  $\mathcal{I}$  in (17). Then, for all initial conditions  $(\bar{r}_0, \bar{\theta}_0) \in \mathcal{I}$ , trajectories asymptotically converge to yield equilibrium radii and phases  $(\bar{r}^*, \bar{\theta}^*) \in \mathcal{I}$  which satisfy:*

$$\frac{\sigma\bar{r}_j^*}{2} - \frac{3\alpha(\bar{r}_j^*)^3}{8} + \kappa \sum_{k=1}^N Y_{jk}\bar{r}_k^* e^{j\bar{\theta}_{jk}^*} = 0, \forall j \in \mathcal{N}. \quad (20)$$

*Proof.* Express (12)–(13) as the gradient flow:

$$\dot{\bar{r}}_j = -\nabla_{\bar{r}_j} V(\bar{r}, \bar{\theta}), \quad (21)$$

$$\dot{\bar{\theta}}_j = -\frac{1}{\bar{r}_j^2} \nabla_{\bar{\theta}_j} V(\bar{r}, \bar{\theta}), \quad (22)$$

where  $V(\bar{r}, \bar{\theta})$  is a potential function given by

$$\begin{aligned} V(\bar{r}, \bar{\theta}) &= \sum_{j=1}^N \varepsilon\omega \int_{\rho=0}^{\bar{r}_j} \left( \frac{3\alpha}{32}\rho^4 - \frac{\sigma}{4}\rho \right) d\rho \\ &\quad - \frac{\varepsilon\omega\kappa}{2} \sum_{j=1}^N \sum_{k=1}^N Y_{jk}\bar{r}_j\bar{r}_k \cos \bar{\theta}_{jk}. \end{aligned}$$

The level sets of  $V(\bar{r}, \bar{\theta})$  are closed (due to continuity), bounded in  $\bar{\theta}$  (due to boundedness of the trigonometric nonlinearities), and radially unbounded in  $\bar{r}$ . The time derivative of  $V(\bar{r}, \bar{\theta})$  along the trajectories of the system is

$$\begin{aligned} \dot{V}(\bar{r}, \bar{\theta}) &= (\nabla_{\bar{r}_j} V(\bar{r}, \bar{\theta}))^T \dot{\bar{r}}_j + \left( \nabla_{\bar{\theta}_j} V(\bar{r}, \bar{\theta}) \right)^T \dot{\bar{\theta}}_j \\ &= -(\nabla_{\bar{r}_j} V(\bar{r}, \bar{\theta}))^2 - \bar{r}_j^2 \left( \frac{1}{\bar{r}_j^2} \nabla_{\bar{\theta}_j} V(\bar{r}, \bar{\theta}) \right)^2 \leq 0. \end{aligned}$$

Therefore, the sublevel sets of  $V(\bar{r}, \bar{\theta})$  are forward invariant. LaSalle's invariance principle [17, Theorem 4.4] and the positive invariance of set  $\mathcal{I}$  can then be invoked to show that the trajectories generated by (12)–(13) converge to the largest positively invariant set contained in

$$\left\{ (\bar{r}, \bar{\theta}) \in \mathcal{I} : V(\bar{r}, \bar{\theta}) \leq V(\bar{r}_0, \bar{\theta}_0), \dot{V}(\bar{r}, \bar{\theta}) = 0 \right\}.$$

Next, we characterize the amplitude and phase equilibria of (12)–(13) (recall that we denote these by vectors  $\bar{r}^*$

and  $\bar{\theta}^*$ , respectively). Setting the derivatives in (12)–(13) to zero, algebraic and trigonometric manipulations allow us to conclude that these are obtained as the solutions of:

$$H + \frac{1}{2}\kappa(E + E^*)\bar{r}^* = 0_N, \quad (23)$$

$$\frac{1}{2j}\kappa(E - E^*)\bar{r}^* = 0_N, \quad (24)$$

where  $H$  is an  $N$ -dimensional vector and  $E$  is an  $N \times N$  complex matrix with entries:

$$\begin{aligned} H_j &= \frac{\sigma\bar{r}_j^*}{2} - \frac{3\alpha(\bar{r}_j^*)^3}{8}, \\ E_{jk} &= \begin{cases} Y_{jj} & \text{if } j = k \\ Y_{jk}e^{j\bar{\theta}_{jk}^*} & \text{if } (j, k) \in \mathcal{E} \\ 0 & \text{otherwise} \end{cases} \end{aligned} \quad (25)$$

It is straightforward to see that the two equations in (23)–(24) boil down to:

$$H + \kappa E\bar{r}^* = 0_N. \quad (26)$$

Expanding out individual entries in the equation above, we recover (20). ■

### C. Local Stability of Phase-synchronous Solutions

In this section, we look at the local exponential stability of equilibria contained in the phase-synchronous set  $\mathcal{S}$  defined in (14).

**Theorem 2 (Local Exponential Stability of Phase-synchronized Equilibria).** *If  $\kappa < 0$ , then phase-synchronized equilibria, defined by*

$$\bar{r}_j^* = \sqrt{\frac{4\sigma}{3\alpha}}, \quad \bar{\theta}_{jk}^* = 0, \quad j, k \in \mathcal{N} \quad (27)$$

*are locally (transversally) exponential stable. Furthermore, with  $\kappa > 0$ , these are locally unstable.*

*Proof.* Linearizing (12)–(13) around (27), we get the Jacobian:

$$\left[ \begin{array}{c|c} -\sigma\omega\varepsilon I_N + \frac{1}{2}\varepsilon\omega\kappa Y & 0 \\ \hline 0 & \sqrt{\frac{3\alpha}{16\sigma}}\varepsilon\omega\kappa Y \end{array} \right]. \quad (28)$$

Since  $Y$  is a Laplacian matrix of a connected graph it is positive semidefinite with  $1_N$  as the only eigenvector in the nullspace which is orthogonal to all the other eigenvectors. Therefore,  $\kappa Y$  (when  $\kappa < 0$ ) has  $N - 1$  negative eigenvalues and consequently the phase-synchronized solutions are locally (transversally) exponentially stable. From the Jacobian, it is also obvious that with  $\kappa > 0$ , we get positive eigenvalues in  $\kappa Y$ . ■

### D. Local Stability of Phase-balanced Solutions

Here, we explore the local exponential stability of equilibria contained in the phase-balanced set,  $\mathcal{B}$ , defined in (15).

**Theorem 3 (Local Exponential Stability of Phase-balanced Set).** *If  $\kappa > 0$  and  $\sigma > \kappa \max(Y_{\text{diag}})$ , then phase-balanced equilibria—where the phases of the oscillators*

evolve functionally constrained as  $\sum_{k=1}^N e^{j\bar{\theta}_k^*} = 0$  and the radii are all equal—are locally exponentially stable. Furthermore, with  $\kappa < 0$ , these are unstable.

*Proof.* Consider the real part of (20) and suppose that all radii are equal. In this case, we see that  $\forall j \in \mathcal{N}$ :

$$\begin{aligned} \frac{\sigma}{2} - \frac{3\alpha(\bar{r}_j^*)^2}{8} &= -\kappa \sum_{k=1}^N Y_{jk} \cos(\bar{\theta}_{jk}^*) \\ &= \kappa \sum_{k=1, (j,k) \in \mathcal{E}}^N \frac{1}{L_{jk}} (\cos \bar{\theta}_{jk}^* - 1) \\ &\leq 0. \end{aligned} \quad (29)$$

Therefore, phase-balanced equilibria with equal radii must satisfy

$$\bar{r}_j^* > \sqrt{\frac{4\sigma}{3\alpha}}, \quad j \in \mathcal{N}. \quad (30)$$

Linearizing (12)–(13) around phase-balanced equilibria, we get the Jacobian:

$$\begin{bmatrix} J^A & J^B \\ 0 & J^D \end{bmatrix}, \quad (31)$$

with entries of  $J^A$  and  $J^D$  given by:

$$\begin{aligned} J_{jk}^A &= \begin{cases} \varepsilon\omega \left( \frac{\sigma}{2} - \frac{9\alpha\bar{r}_j^{*2}}{8} \right) + \frac{\varepsilon\omega\kappa}{2} Y_{jj} & \text{if } j = k \\ \frac{\varepsilon\omega\kappa}{2} Y_{jk} \cos \bar{\theta}_{jk}^* & \text{if } j \neq k \end{cases} \\ J_{jk}^D &= \begin{cases} -\frac{\varepsilon\omega\kappa}{2\bar{r}_j^*} Y_{jj} & \text{if } j = k \\ \frac{\varepsilon\omega\kappa}{2\bar{r}_j^*} Y_{jk} \cos \bar{\theta}_{jk}^* & \text{if } j \neq k \end{cases}. \end{aligned} \quad (32)$$

From (30) and the entries spelled out in (32), we see that both  $J^A$  and  $J^D$  are diagonally dominant with negative entries on their respective diagonals when  $\kappa > 0$  and  $\sigma > \kappa \max(Y_{\text{diag}})$  yielding phase-balanced solutions that are locally exponentially stable. By the same token, when  $\kappa < 0$ , we see that these are unstable. ■

## IV. NUMERICAL SIMULATION RESULTS

### A. Parameters

We simulate a system of 10 identical Van der Pol oscillator circuits connected at nodes of a cycle graph with identical inductances and resistances. The inductances of the lines are chosen to be  $L = 100\text{mH}$  and resistances are chosen to be  $R = 0.1\Omega$ . This yields  $\lambda_{\max}(Y) = 400$  and  $\max(Y_{\text{diag}}) = 20$  for the cycle network. The parameters of the oscillators are chosen as follows:  $\varepsilon = 0.01, \sigma = 60\text{S}, \alpha = 80, \omega = 100\text{rad/s}$ .

### B. Simulation

For the time-domain simulation, we begin with  $\kappa = -0.2$  for time  $0 \leq t \leq 1\text{sec}$ , switch to  $\kappa = 0.2$  for time  $1\text{sec} < t \leq 4\text{sec}$ , and revert to  $\kappa = -0.2$  for time  $4\text{sec} < t \leq 6\text{sec}$ . The positive-invariance condition (16), i.e.,  $\sigma > -\kappa\lambda_{\max}(Y)$  is satisfied for both values of  $\kappa$ . Furthermore, for  $\kappa = -0.2$  it can be verified that  $\sigma > \kappa \max(Y_{\text{diag}})$ . Figures 4 and 5 depict the evolution of the averaged phases and amplitudes of the oscillators through the above simulation. For the period

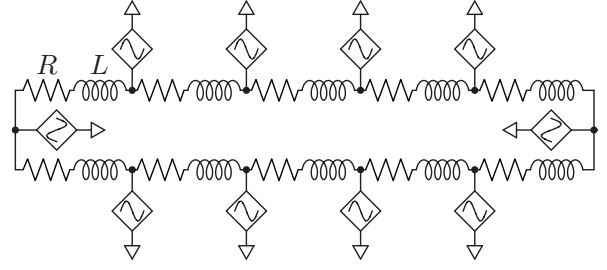


Fig. 3: Topology utilised in the simulations: Van der Pol oscillators (illustrated with the shorthand notation established in Fig. 2) in an electrical network with a cycle graph topology. All transmission lines have the same resistance (denoted by  $R$ ), and the same inductance (denoted by  $L$ ).

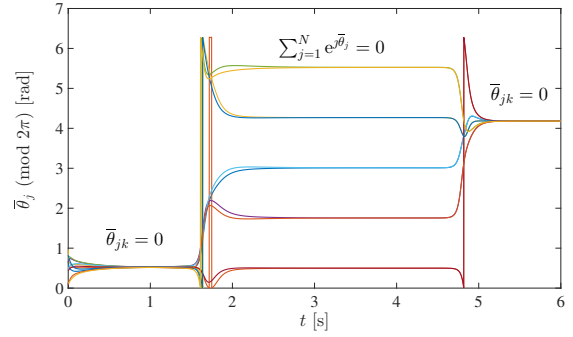


Fig. 4: Evolution of phases for the time-domain simulation. We set  $\kappa = -0.2$  for  $0 \leq t \leq 1\text{sec}$  during which the phases synchronize; switch to  $\kappa = 0.2$  for  $1\text{sec} < t \leq 4\text{sec}$  during which the phases are balanced; revert to  $\kappa = -0.2$  for  $4\text{sec} < t \leq 6\text{sec}$  and they synchronize again.

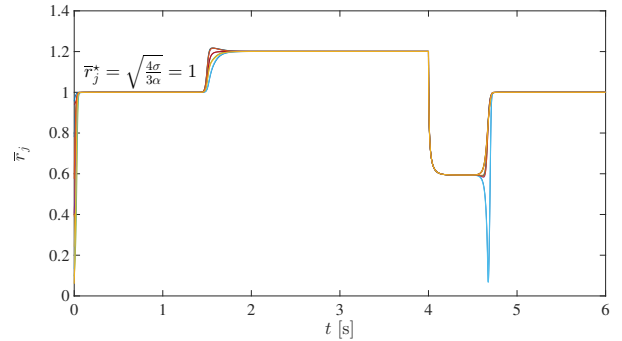


Fig. 5: Evolution of amplitudes for the time-domain simulation. We set  $\kappa = -0.2$  for  $0 \leq t \leq 1\text{sec}$  during which amplitudes satisfy constraint (27); switch to  $\kappa = 0.2$  for  $1\text{sec} < t \leq 4\text{sec}$  during which amplitudes satisfy constraint (30); and revert to  $\kappa = -0.2$  for  $4\text{sec} < t \leq 6\text{sec}$  when amplitudes settle to (27) again.

of time when the feedback gain,  $\kappa = -0.2$ , the phases of the oscillators are all synchronized, and the radii are all equal and satisfy (27). Similarly, when the feedback gain  $\kappa = 0.2$ , the phases are functionally constrained by  $\sum_{k=1}^{10} e^{j\bar{\theta}_k^*} = 0$ , and furthermore, the amplitudes satisfy the constraint (30).

## V. CONCLUSIONS AND DIRECTIONS FOR FUTURE WORK

We presented a unified analytical approach to examine the stability for phase-balancing and phase-synchronization in networks of identical Van der Pol oscillators connected in a uniform electrical network. Our results uncovered the relationship between the sign of the feedback and the local exponential stability of the two types of motions. As part of future work, one could extend the results here to the setting of heterogeneous networks (with no uniformity assumptions on transmission lines) and oscillators (with different natural resonant frequencies).

## ACKNOWLEDGEMENTS

The work of M. Sinha and S. Dhople was supported by the National Science Foundation through awards 1453921 and 1509277.

## REFERENCES

- [1] F. Dörfler and F. Bullo, "Synchronization in complex networks of phase oscillators: A survey," *Automatica*, vol. 50, no. 6, pp. 1539–1564, 2014.
- [2] L. A. B. Törres, J. P. Hespanha, and J. Moehlis, "Synchronization of identical oscillators coupled through a symmetric network with dynamics: A constructive approach with applications to parallel operation of inverters," *IEEE Transactions on Automatic Control*, vol. 60, no. 12, pp. 3226–3241, December 2015.
- [3] B. B. Johnson, S. V. Dhople, A. O. Hamadeh, and P. T. Krein, "Synchronization of nonlinear oscillators in an LTI electrical power network," *IEEE Transactions on Circuits and Systems I: Regular Papers*, vol. 61, no. 3, pp. 834–844, March 2014.
- [4] M. Li, Y. Gui, J. C. Vasquez, and J. M. Guerrero, "Adaptive synchronization of grid-connected three-phase inverters by using virtual oscillator control," in *2018 IEEE Applied Power Electronics Conference and Exposition (APEC)*, March 2018, pp. 1130–1135.
- [5] M. Colombino, D. Groß, and F. Dörfler, "Global phase and voltage synchronization for power inverters: a decentralized consensus-inspired approach," in *56th Annual IEEE Conference on Decision and Control (CDC)*, December 2017, pp. 5690–5695.
- [6] D. F. Frost and D. A. Howey, "Completely decentralized active balancing battery management system," *IEEE Transactions on Power Electronics*, vol. 33, no. 1, pp. 729–738, January 2018.
- [7] T. Wang and J. Roychowdhury, "Oscillator-based Ising machine," 2017. [Online]. Available: <http://arxiv.org/abs/1709.08102>
- [8] T. Wang, "Achieving phase-based logic bit storage in mechanical metronomes," 2017. [Online]. Available: <http://arxiv.org/abs/1710.01056>
- [9] J. Roychowdhury, "Boolean computation using self-sustaining nonlinear oscillators," *Proceedings of the IEEE*, vol. 103, no. 11, pp. 1958–1969, November 2015.
- [10] M. Sinha, J. Poon, B. Johnson, M. Rodriguez, and S. V. Dhople, "Decentralized interleaving of parallel-connected buck converters," *IEEE Transactions on Power Electronics*, 2018, to appear.
- [11] M. Sinha, F. Dörfler, B. B. Johnson, and S. V. Dhople, "Synchronization of Liénard-type oscillators in uniform electrical networks," in *2016 American Control Conference (ACC)*, July 2016, pp. 4311–4316.
- [12] M. Sinha, F. Dörfler, B. B. Johnson, and S. V. Dhople, "Synchronization of Liénard-type oscillators in heterogeneous electrical networks," in *2018 Indian Control Conference (ICC)*, January 2018, pp. 240–245.
- [13] M. Sinha, F. Dörfler, B. Johnson, and S. Dhople, "Phase balancing in globally connected networks of Liénard oscillators," in *2017 IEEE 56th Annual Conference on Decision and Control (CDC)*, December 2017, pp. 595–600.
- [14] L. Scardovi, A. Sarlette, and R. Sepulchre, "Synchronization and balancing on the N-torus," *Systems & Control Letters*, vol. 56, no. 5, pp. 335 – 341, 2007.
- [15] R. Sepulchre, D. A. Paley, and N. E. Leonard, "Stabilization of planar collective motion with limited communication," *IEEE Transactions on Automatic Control*, vol. 53, no. 3, pp. 706–719, April 2008.
- [16] S. E. Tuna, "Synchronization analysis of coupled Liénard-type oscillators by averaging," *Automatica*, vol. 48, no. 8, pp. 1885–1891, 2012.
- [17] H. Khalil, *Nonlinear Systems*, 3rd ed. Upper Saddle River, NJ: Prentice Hall, 2002.
- [18] J. W. Swift, S. H. Strogatz, and K. Wiesenfeld, "Averaging of globally coupled oscillators," *Physica D: Nonlinear Phenomena*, vol. 55, no. 3-4, pp. 239–250, 1992.